

Supercooling of the disordered vortex lattice in $\text{Bi}_2\text{Sr}_2\text{CaCu}_2\text{O}_{8+\delta}$

C.J. van der Beek¹, S. Colson¹, M.V. Indenbom^{1,2}, and M. Konczykowski¹

¹*Laboratoire des Solides Irradiés, Ecole Polytechnique, 91128 Palaiseau, France*

²*Institute of Solid State Physics, 142432 Chernogolovka, Moscow District, Russia*

(September 10, 1999)

Time-resolved local induction measurements near to the vortex lattice order-disorder transition in optimally doped $\text{Bi}_2\text{Sr}_2\text{CaCu}_2\text{O}_{8+\delta}$ single crystals shows that the high-field, disordered phase can be quenched to fields as low as half the transition field. Over an important range of fields, the electro-dynamical behavior of the vortex system is governed by the co-existence of the two phases in the sample. We interpret the results in terms of supercooling of the high-field phase and the possible first order nature of the order-disorder transition at the “second peak”.

It is now well accepted that the mixed state in type II superconductors is itself subdivided into different vortex phases. In very clean materials, notably single crystals of the high- T_c -cuprates $\text{YBa}_2\text{Cu}_3\text{O}_{7-\delta}$ [1] and $\text{Bi}_2\text{Sr}_2\text{CaCu}_2\text{O}_{8+\delta}$ [2–4], the vortex lattice, characterized by long-range translational and orientational order, undergoes a first order transition (FOT) to a flux liquid state without long-range order [5]. The FOT is observed at inductions B at which vortex pinning by crystalline defects is negligible and the vortex system can rapidly relax to thermodynamic equilibrium [3,6], but which are still much below the upper critical field B_{c2} . The FOT is prolonged into the low temperature regime of nonlinear vortex response by a transition from the weakly pinned low-field vortex lattice to a strongly pinned, disordered high-field vortex phase [4,7,8]. This order-disorder transition is manifest through the so-called “second peak” feature in the magnetic hysteresis loops, a result of the dramatic increase of the sustainable shielding current associated with bulk pinning [4,9–11]. It was proposed that the crossover from the FOT to the “second peak” regime constitutes a critical point in the phase diagram [3,12], which in $\text{Bi}_2\text{Sr}_2\text{CaCu}_2\text{O}_{8+\delta}$ would lie near $T \approx 40$ K. In more dirty type-II superconductors the FOT and the critical point are absent and the critical current “peak effect” is found at temperatures up to T_c [13]. The peak effect is often accompanied by strongly history dependent dynamical behavior of the vortex system at fields and temperatures just below it, suggesting that a first order transition lies at its origin [14–16].

Among the abovementioned materials the layered superconductor $\text{Bi}_2\text{Sr}_2\text{CaCu}_2\text{O}_{8+\delta}$ has a specific interest: its high Ginzburg number $Gi \sim 0.01$ means that vortex lines are extremely sensitive to thermal and static fluctuations and that the FOT and second-peak lines are depressed to inductions lower than 1 kG. The local induction and flux dynamics around the transition can then be accurately measured using local Hall-array magnetometry [3,4,10,11] and magneto-optics. Recently, the decomposition of the vortex system near the FOT in $\text{Bi}_2\text{Sr}_2\text{CaCu}_2\text{O}_{8+\delta}$ into coexisting lattice and liquid

phases was imaged using this latter technique [17]. In this Letter, we image the flux dynamics and the coexistence of the two *pinned* vortex phases in $\text{Bi}_2\text{Sr}_2\text{CaCu}_2\text{O}_{8+\delta}$ near the disordering transition at the “second peak”. In particular, we find that the disordered phase can be quenched to flux densities that are nearly half that at which it exists in equilibrium. We interpret our results in terms of supercooling of the high field phase. This suggests that the order-disorder transition at the second peak is of first order, and that it is the “true” continuation of the FOT in the regime of slow vortex dynamics. By implication, we propose that a putative critical point lies at a temperature not exceeding 14 K.

The experiments were performed on an optimally doped $\text{Bi}_2\text{Sr}_2\text{CaCu}_2\text{O}_{8+\delta}$ single crystal ($T_c = 90$ K) of size $630 \times 250 \times 35 \mu\text{m}^3$, grown at the University of Tokyo using the travelling-solvent floating zone technique, and selected for its uniformity. Previous experiments on this crystal using the Hall-probe array technique have revealed the disordering transition of the vortex lattice to occur at $B_{sp} = 380$ G [11]. We have visualized the flux density distribution at inductions close to the transition using the technique of Ref. [18]. A ferrimagnetic garnet film with in-plane anisotropy is placed directly on top of the crystal, and observed using linearly polarized light. The induction component perpendicular to the film induces a perpendicular magnetization and concomitant Faraday rotation of the polarization, which is then visualized using an analyzer. The local induction-variations induced by the presence of the superconducting crystal are revealed as intensity variations of the reflected light, the brighter regions corresponding to the greater flux, or vortex, density. The technique is particularly useful for the study of the low-field behavior of oxide superconductors, in which the measurement of the electromagnetic response of the vortex system is easily marred by the presence of surface barriers [19,20], the appearance of the Meissner phase [21,22], and macroscopic defects [23,24]. The direct mapping of the flux density allows one to distinguish where currents flow inside the superconductor [25], to identify inhomogeneous parts of

the crystal, and, eventually, to eliminate them.

Figure 1(a) shows a magneto-optical image of the crystal after zero-field cooling to $T = 24.6$ K and the slow ramp of the applied magnetic field H_a to 486 G. There is a bright belt around the crystal edge, corresponding to a region of high field gradient, and, visible under the sawtooth-like magnetic domain wall structure in the garnet, an inner region with little contrast, indicating a plateau in the local induction. The axis of the sawtooth structure is located there where the induction component parallel to the garnet film vanishes [26]. This corresponds to the boundary between regions of zero and non-zero screening current in the $\text{Bi}_2\text{Sr}_2\text{CaCu}_2\text{O}_8$ crystal. We infer that no current flows in the central region of (nearly) constant induction. Conversion of the light intensity to flux density shows that the plateau induction equals that expected at the transition, $B_{sp} = 380$ G.

The evolution of the flux profiles at successive values of the applied field during the ramp is shown in Fig. 1(b). At small H_a , one has a comparatively large step in the induction at the crystal edges, and a dome-shaped flux distribution in the crystal interior. Such a flux profile occurs when the edge screening current due to a surface barrier is much greater than the bulk shielding current, which is the result of vortex pinning [19,20]. The dome-like profile moves up to higher induction values as field is increased: its evolution stops when the induction in the crystal

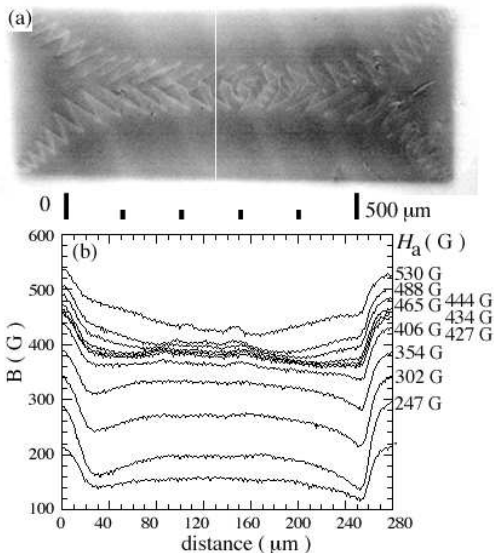


FIG. 1. (a) Magneto-optical image of the flux distribution on the surface of the $\text{Bi}_2\text{Sr}_2\text{CaCu}_2\text{O}_8$ crystal after zero-field cooling to $T = 24.6$ K and the slow application of an external field $H_a = 486$ G. (b) Profiles of the magnetic induction at successive values of the external field during the field ramp, taken along the white line in (a). The step in the induction at either edge of the crystal is the result of the surface barrier screening current [19]. The small irregularities in the center are due to the presence of magnetic domain walls in the garnet film, visible as the “sawtooth” structures in (a).

H_a is increased further, the flux profile flattens out, *i.e.* B becomes constant throughout the crystal as the high-field vortex phase spreads outwards from the crystal center. As a result, the slope $\partial B/\partial H_a$ becomes equal to the Meissner slope [11]. At $H_a = 444$ G, the whole crystal is in the high-field state, and new flux (vortices) penetrates from the edges; it cannot, however, accumulate in the crystal center but adopts the linear gradient characteristic of the pinning-induced critical state [27]. This indicates that, at this temperature, field, and field ramp rate, the pinning current is comparable to or greater than the surface barrier current, giving rise to the “second peak feature” in the magnetic moment [4,7,11].

Figure 2(a) shows the relaxation of the flux profile after a rapid decrease of the applied field from 500 G to 120 G, at $T = 23$ K. The initial flux profile is similar to the one for $H_a = 488$ G in Fig. 1: the “critical state” fronts of the high-field phase have not yet penetrated the whole crystal so that the induction in the crystal center is nearly constant $B \gtrsim B_{sp}$; Thus, the internal induction is lower than the applied field because of the combined screening by the surface barrier current [19,20] and by the high-field phase. When H_a is suddenly decreased, the sample initially fully screens the field change ($t = 0.16$ s). From $t \gtrsim 0.32$ s onwards, vortices leave the sample. The flux

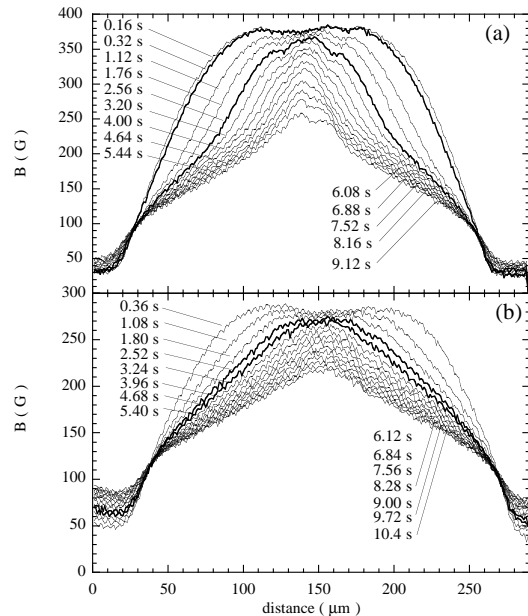


FIG. 2. (a) Relaxation of the flux profile on the surface of the $\text{Bi}_2\text{Sr}_2\text{CaCu}_2\text{O}_8$ crystal at $T = 23.0$ K after the application of an external field $H_a^{max} = 500$ G and its successive rapid decrease to 120 G. The profiles display three slopes $\partial B_z/\partial x$, corresponding to the surface barrier screening current (near the edges at $30 \mu\text{m}$ and $260 \mu\text{m}$) [19], and to bulk screening currents in the low-field and high-field vortex phases, respectively. (b) The same, but after field-cooling from $T = 28$ K in $H_a^{max} = 383$ G. The profiles are composed of two linear sections corresponding to the surface barrier current and the relaxing critical state established in the low-field phase *only*.

profiles display three distinct linear sections with different gradients, corresponding to three mechanisms opposing vortex motion and exit. The gradient nearest to the crystal edge corresponds to the surface barrier current [19,20]; the two gradients in the bulk correspond to the (rapidly decaying) screening current in the low-field vortex lattice phase and the (nearly constant) current in the high-field disordered vortex phase, respectively. The phase transformation line, at which one passes from the low-field to the high field current, progressively moves to the crystal center, until the whole crystal is in the low-field phase at $t \gtrsim 10$ s. We note that these features are not observed if one prepares a similar initial flux profile with a central plateau of $B < B_{sp}$ (Fig. 2(b)). There are then only *two* flux gradients corresponding to the surface barrier and the screening current in the low-field phase. These results unambiguously demonstrate that the region of constant flux density B_{sp} in the sample center, obtained during a slow field ramp (Fig. 1), is in the high-field phase; namely, it responds to an external field perturbation by developing the corresponding, “high-field”, screening current. Moreover, the screening current at any point in the crystal *depends on the history* of the vortex system. This is well seen at *e.g.* $x = 100 \mu\text{m}$ and $B = 250$ G: if this induction is attained by a rapid quench from the high-field phase, the screening current is equal to that usually observed for $B > B_{sp}$. If, during the experiment, the vortex system did not undergo the phase transformation to the disordered state, a screening current characteristic of the low-field phase is observed.

A glance at the flux density scale on Fig. 2 shows that the disordered vortex phase in the center of the crystal, identifiable in Fig. 2(a) by the large screening current it can sustain, has in fact been quenched to inductions nearly half B_{sp} . A similar situation occurs if one rapidly increases the magnetic field from zero to a value much

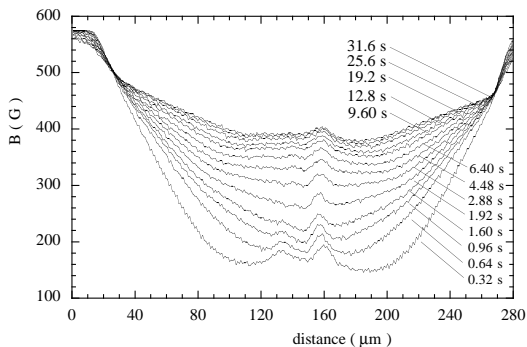


FIG. 3. Relaxation of the induction profile on the surface of the $\text{Bi}_2\text{Sr}_2\text{CaCu}_2\text{O}_8$ at $T = 23.0$ K after the sudden application of an external field $H_a^{max} = 537$ G. For $t > 0.96$ s, the flux profiles display three slopes $\partial B_z / \partial x$, corresponding to the surface barrier current, and bulk screening currents in the high-field (outer) and low-field (inner) vortex phases, respectively. The irregularities near the center are again due to the presence of domain walls in the garnet film.

above B_{sp} (Fig. 3). Initially, the crystal again perfectly screens the field change. As vortices enter the crystal, they are initially in the disordered state. Only when they move sufficiently far into the interior does the phase transformation to the ordered vortex lattice state take place. The decrease of the flux density from $B \approx \mu_0 H_a > B_{sp}$ at the crystal edge to $B \ll B_{sp}$ inside the sample due to formation of the critical state necessitates the presence of the phase transformation line in the sample interior. This is visible in Fig. 3 as the changes in the induction gradient near 80 and 220 μm . The induction at which the transformation takes place is again lower than B_{sp} , *i.e.* the high field phase is now quenched as it penetrates from the sample edge, in this case to an induction ~ 200 G. As the induction gradient in the high field phase relaxes due to thermally activated flux motion, the phase transformation line moves from the crystal edges towards the crystal centre. In contrast to the dramatic quenching of the disordered phase, we did not, in any experiment, obtain unambiguous indications that the low field state can be prepared at $B > B_{sp}$.

The above observations have important implications for the vortex phase diagram in $\text{Bi}_2\text{Sr}_2\text{CaCu}_2\text{O}_{8+\delta}$ and other layered superconductors. First of all, it is shown that the phase transition line between the low-field lattice phase and the high-field disordered vortex phase is, to within our spatial resolution ($\sim 10 \mu\text{m}$), sharp, and that its position can be readily identified by the difference in shielding current density developed by the two phases after a field perturbation. The phase transformation line can, depending on the ratio of these currents, move inwards from the crystal edge, which happens at relatively low temperature or large field sweep rates (Figs. 2 and 3), or outwards from the crystal center, at higher temperatures near the reported “critical point” [3] or during slow field ramps (such as in Fig. 1). In the latter case, any small “external” field perturbation is screened by the high current developed by the disordered vortex phase, so that the induction in the crystal center is held constant and equal to B_{sp} (as in Fig. 1). This notably holds for the induction change ΔB associated with the entropy change $\Delta S = (1/\Delta B)\partial H_m/\partial T$ at the FOT [3] (H_m is the FOT field). Thus, our results give a natural explanation for the apparent vanishing of ΔS at a nonzero temperature, without the need to invoke the presence of a critical point in the phase diagram. It is not ΔS that vanishes at $T \sim 40$ K, but the corresponding change ΔB of the equilibrium flux density which cannot be observed, because it is perfectly screened by the pinning “critical” current developed in the disordered high-field phase. In other words, thermodynamic equilibrium can no longer be achieved, because, for $T \lesssim 40$ K [28], the high-field phase is pinned on the typical experimental time scale. The extra vortices needed to satisfy the constitutive relation $B(H)$ cannot enter the region where the high-field phase is present.

Further support for the absence of a critical point near 40 K is given by the quenching experiments of Figs. 2(a) and 3. The flux distributions shown in these plots correspond to the coexistence of the ordered low-field vortex lattice state and the disordered high-field phase. The latter is *metastable* since it exists at inductions that are much smaller than B_{sp} . We interpret this observation as *supercooling* of the disordered state, which in turn suggests that the transition at B_{sp} is of first order. Further, the continuity with the high-temperature FOT [4] implies that it is simply the continuation of the “lattice-to-liquid” transition into the regime of slow vortex dynamics. The observation of the present features at temperatures down to 14 K, below which the “second peak” cannot be observed at ordinary experimental timescales, means that if a critical point exists, it should lie *below* this temperature. This would be in agreement with the high-field vortex glass transition line of Ref. [29]. The low-field extrapolation of this line, was found to interrupt B_{sp} around the same temperature.

Finally we point out the consequences for measurements of flux dynamics. The possibility of phase coexistence should be taken into account in low-field magnetic relaxation experiments, especially those triggered by a decrease in the applied magnetic field. In such experiments, the decay rate of the global magnetic moment and of the local induction will be determined by no less than four contributions: the relaxation of the surface barrier current, flux creep in the low-field and high-field vortex phase, and the rate at which the vortex lattice recrystallizes at the phase transformation line. At temperatures below 20 K, these processes become slow and similarly impede flux transport. Supercooling of a disordered vortex phase has been previously observed in other type-II superconductors such as α - Nb_3Ge [14] and NbSe_2 [15]. The anomalous flux dynamics observed in the field regime close to but below the critical current peak [16] may find a natural explanation in the “asymmetric” vortex response and flux profiles introduced in transport measurements by phase coexistence and the supercooling phenomenon.

In conclusion, we have visualized the flux distribution in the “second peak” regime in $\text{Bi}_2\text{Sr}_2\text{CaCu}_2\text{O}_8$. The peak effect feature, the fact that $\partial M/\partial H_a = -1$ below the peak, and the vanishing of ΔB associated with the FOT at $T \sim 40$ K are the result of the pinning current in the high field phase, which prohibits flux entry into this phase until the phase transformation is complete. We have observed supercooling of the high-field disordered vortex system to fields nearly half the phase transformation field B_{sp} . The results suggest that the vortex order-disorder transition at the second peak in $\text{Bi}_2\text{Sr}_2\text{CaCu}_2\text{O}_8$ is first order, and that any critical point in the phase diagram lies below 14 K.

We thank N. Motohira for providing the $\text{Bi}_2\text{Sr}_2\text{CaCu}_2\text{O}_8$ crystal, and M.V. Feigel'man, P.H. Kes,

A. Soibel, A. Sudbø, and E. Zeldov for fruitful discussions.

-
- [1] H. Safar *et al.*, Phys. Rev. Lett. **69**, 824 (1992); W.K. Kwok *et al.*, Phys. Rev. Lett. **69**, 3370 (1992).
 - [2] H. Pastoriza *et al.*, Phys. Rev. Lett. **72**, 2951 (1994).
 - [3] E. Zeldov *et al.*, Nature **375**, 373 (1995).
 - [4] B. Khaykovich *et al.*, Phys. Rev. Lett. **76**, 2555 (1996).
 - [5] R. Cubitt *et al.*, Nature **365**, 410 (1993).
 - [6] A. Schilling *et al.*, Nature **382**, 791 (1996).
 - [7] R. Cubitt *et al.*, Physica C **235–240**, 2583 (1994).
 - [8] T. Nishizaki, T. Naito, and N. Kobayashi, Physica (Amsterdam) C **282–287**, 2117 (1997); K. Deligiannis *et al.*, Phys. Rev. Lett. **79**, 2121 (1997).
 - [9] N. Chikumoto *et al.*, Phys. Rev. Lett. **69**, 1260 (1992).
 - [10] D. Majer, E. Zeldov, H. Shtrikman, and M. Konczykowski, in: *Coherence in High Temperature Superconductors*, Edited by G. Deutscher and A. Revcolevschi (World Scientific, 1996).
 - [11] S. Berry *et al.*, Physica C **282–287**, 2259(1997).
 - [12] H. Safar *et al.*, Phys. Rev. Lett. **70** 3800, (1993).
 - [13] P. Koorevaar *et al.*, Phys. Rev. B **42**, 1004 (1990); S. Bhattacharya and M.J. Higgins, Phys. Rev. Lett. **70**, 2617 (1993); G. D’Anna, M.-O. André, and W. Benoit, Europhys. Lett. **25**, 539 (1994); R. Modler *et al.*, Phys. Rev. Lett. **76**, 1292 (1996); D. Giller *et al.*, Phys. Rev. Lett. **79**, 2542(1997); M. Pissas *et al.*, Phys. Rev. B **59**, 12121 (1999); S. Anders *et al.*, Phys. Rev. B **59**, 13635 (1999).
 - [14] R. Wördenweber and P.H. Kes, Phys. Rev. B **34**, 494 (1986).
 - [15] W. Henderson, E.Y. Andrei, M.J. Higgins, and S. Bhattacharya, Phys. Rev. Lett. **77**, 2077 (1996); S.B. Roy and P. Chaddah, J. Phys.: Condens. Matter **9**, L625 (1997); G. Ravikumar *et al.*, Phys. Rev. B **57**, R11069 (1998); S.S. Banerjee *et al.*, Phys. Rev. B **58**, 995 (1998).
 - [16] W. Henderson, E.Y. Andrei, and M.J. Higgins, Phys. Rev. Lett. **81**, 2353 (1998).
 - [17] A. Soibel *et al.*, preprint (1999).
 - [18] L.A. Dorosinskiĭ *et al.*, Physica C **203**, 149 (1992).
 - [19] M.V. Indenbom *et al.*, in: *Proceedings of the 7th Int. Workshop on Critical Currents in Superconductors*, Alpbach, Austria, Jan. 24–27, 1994, Edited by H.W. Weber (World Scientific, 1994).
 - [20] E. Zeldov *et al.*, Phys. Rev. Lett. **73**, 1428 (1994).
 - [21] M.V. Indenbom *et al.*, Phys. Rev. B **51**, 15484 (1995).
 - [22] V.K. Vlasko-Vlasov *et al.*, Phys. Rev. B **56**, 5622 (1997).
 - [23] Th. Schuster *et al.*, Phys. Rev. B **52**, 10375 (1995).
 - [24] M.R. Koblischka *et al.*, Physica C **249**, 339 (1995).
 - [25] U. Welp, *et al.*, Nature **376**, 44 (1995).
 - [26] M.V. Indenbom, H. Kronmüller, T.W. Li, P.H. Kes, and A.A. Menovsky, Physica (Amsterdam) C **226**, 325 (1994).
 - [27] C.P. Bean, Phys. Rev. Lett. **8**, 250 (1962).
 - [28] D. Fuchs *et al.*, Phys. Rev. Lett. **80**, 4971 (1998).
 - [29] C.J. van der Beek *et al.*, Physica C **195**, 307 (1992).